

# UC Irvine

## UC Irvine Previously Published Works

### Title

Aqp0a Regulates Suture Stability in the Zebrafish Lens

### Permalink

<https://escholarship.org/uc/item/2zp1f7w3>

### Journal

Investigative Ophthalmology & Visual Science, 59(7)

### ISSN

0146-0404

### Authors

Vorontsova, Irene  
Gehring, Ines  
Hall, James E  
[et al.](#)

### Publication Date

2018-06-04

### DOI

10.1167/iovs.18-24044

### Copyright Information

This work is made available under the terms of a Creative Commons Attribution License, available at <https://creativecommons.org/licenses/by/4.0/>

Peer reviewed

# Aqp0a Regulates Suture Stability in the Zebrafish Lens

Irene Vorontsova,<sup>1,2</sup> Ines Gehring,<sup>2</sup> James E. Hall,<sup>1</sup> and Thomas F. Schilling<sup>2</sup>

<sup>1</sup>Department of Physiology and Biophysics, University of California, Irvine, California, United States

<sup>2</sup>Department of Developmental and Cell Biology, University of California, Irvine, California, United States

Correspondence: Thomas F. Schilling, Department of Developmental and Cell Biology, 4462 Natural Sciences 2, University of California, Irvine, CA 92697-2300, USA; tschilli@uci.edu.

Submitted: February 7, 2018

Accepted: April 19, 2018

Citation: Vorontsova I, Gehring I, Hall JE, Schilling TF. Aqp0a regulates suture stability in the zebrafish lens.

*Invest Ophthalmol Vis Sci.*

2018;59:2869–2879. <https://doi.org/10.1167/iovs.18-24044>

**PURPOSE.** To investigate the roles of Aquaporin 0a (Aqp0a) and Aqp0b in zebrafish lens development and transparency.

**METHODS.** CRISPR/Cas9 gene editing was used to generate loss-of-function deletions in zebrafish *aqp0a* and/or *aqp0b*. Wild type (WT), single mutant, and double mutant lenses were analyzed from embryonic to adult stages. Lens transparency, morphology, and growth were assessed. Immunohistochemistry was used to map protein localization as well as to assess tissue organization and distribution of cell nuclei.

**RESULTS.** *aqp0a*<sup>-/-</sup> and/or *aqp0b*<sup>-/-</sup> cause embryonic cataracts with variable penetrance. While lenses of single mutants of either gene recover transparency in juveniles, double mutants consistently form dense cataracts that persist in adults, indicating partially redundant functions. Double mutants also reveal redundant Aqp0 functions in lens growth. The nucleus of WT lenses moves from the anterior pole to the lens center with age. In *aqp0a*<sup>-/-</sup> mutants, the nucleus fails to centralize as it does in WT or *aqp0b*<sup>-/-</sup> lenses, and in double mutant lenses there is no consistent lens nuclear position. In addition, the anterior sutures of *aqp0a*<sup>-/-</sup>, but not *aqp0b*<sup>-/-</sup> mutants, are unstable resulting in failure of suture maintenance at older stages and anterior polar opacity.

**CONCLUSIONS.** Zebrafish Aqp0s have partially redundant functions, but only Aqp0a promotes suture stability, which directs the lens nucleus to centralize, failure of which results in anterior polar opacity. These studies support the hypothesis that the two Aqp0s subfunctionalized during fish evolution and that Aqp0-dependent maintenance of the anterior suture is essential for lens transparency.

**Keywords:** AQP0, lens, zebrafish, *Danio rerio*, cataract

AQP0 is the most abundant lens membrane protein and is essential for lens development and transparency. Mutations in AQP0 lead to cataract formation in humans, mice, and rats.<sup>1</sup> Thus, understanding the normal functions of AQP0 and their disruption in disease could lead to the development of treatments to prevent or delay the leading cause of worldwide blindness.

Mammalian AQP0 exhibits multiple functions in lens fiber cells including water transport (see Ref. 2 for review), adhesion,<sup>3</sup> anchoring cytoskeletal proteins to the intermediate filament protein filensin,<sup>4,5</sup> and regulating connexin 50 function in gap junctions.<sup>6,7</sup> Ultimately, these roles all contribute to the generation of the lens refractive index gradient.<sup>8</sup>

The regulation of AQP0 water permeability has been extensively studied in the *Xenopus laevis* oocyte expression system by measuring permeability in response to hypotonic stress. Site-directed mutagenesis identified the residues crucial for pH<sup>9</sup> and Ca<sup>2+</sup> regulation,<sup>10,11</sup> effects of phosphorylation on permeability<sup>12</sup> and consequences of the C-terminal truncation that normally occurs in mature lens fiber cells.<sup>8,13</sup> In vitro tests have similarly identified amino acids required for adhesion.<sup>14,15</sup> Because multiple functions reside in the single mammalian AQP0, it is difficult to separate the requirements for each function experimentally in a mammal. Apparent subfunctionalization of two Aqp0s in zebrafish provides an opportunity to overcome this difficulty.

Because of an ancient teleost-lineage genome duplication, zebrafish (*Danio rerio*) have two orthologs of AQP0, *aqp0a*, and *aqp0b*.<sup>16</sup> Morpholino (MO) knockdown of expression of either gene leads to cataract formation at 3 days post-fertilization (dpf),<sup>17</sup> which can be self- but not cross-rescued.<sup>18</sup> Thus, both *aqp0a* and *aqp0b* are essential for embryonic lens transparency. They share 85% amino acid identity but diverge in key amino acids crucial for pH regulation of water permeability.<sup>17</sup> Aqp0a expressed in *Xenopus laevis* oocytes shows increased permeability with basic pH, while Aqp0b shows increased permeability with acidic pH.<sup>19</sup> Interestingly, it also appears that there are nonwater-permeable variants of Aqp0b (G19S).<sup>17,19</sup> The fact that water permeability of Aqp0b is not essential for normal embryonic lens transparency is also supported by DNA-construct rescue of *aqp0b* knockdown by a mutant version of MIPfun (N68Q) lacking water permeability (MIPfun is an AQP0 in killifish).<sup>18</sup> These data suggest that Aqp0a and Aqp0b have functionally diverged and that water transport is an essential characteristic of Aqp0a, but not of Aqp0b.

Zebrafish lens secondary fiber cells elongate, migrate from the developing bow region by 28 hours postfertilization, and extend bidirectionally.<sup>20</sup> Their anterior tips migrate toward the center of the lens epithelium, while their posterior tips migrate toward the center of the lens capsule. These fiber cell tips eventually detach from the anterior epithelium or posterior capsule at the poles and interlock end-to-end with opposing fiber cell tips to form the sutures.<sup>21</sup>

Sutures extend from the embryonic nucleus, comprised of primary fiber cells, to the epithelium at the anterior pole, and to the lens capsule at the posterior pole. The zebrafish lens has a very simple suture architecture, with umbilical or point sutures, formed from crescent-shaped secondary fiber cells that are wider at their centers and taper at their ends to meet at the sutures.<sup>22</sup>

Suture formation requires a polarity signal in fiber cells that involves asymmetrically localized planar cell polarity (PCP) proteins,<sup>23</sup> while the primary cilium is nonessential for mouse anterior suture formation.<sup>24</sup> Mutations in the PCP genes *Van Gogh-like 2* and *Celsr1* perturb suture formation.<sup>25</sup> A lens-fiber basal membrane complex, enriched in F-actin, integrin $\beta$ 1 (Itg $\beta$ 1) and E-cadherin, rearranges in the final stages of migration and detaches from the capsule to form the posterior suture in rat lenses.<sup>25</sup> Additionally, migration of elongating fiber cells in zebrafish requires Itg $\alpha$ 5 and fibronectin (Fn1).<sup>26</sup>

The exact role of AQP0 in the formation or maintenance of lens sutures is unknown. However, SEM analysis in AQP0-deficient heterozygous mouse lenses has shown that posterior fiber cells have abnormally large tips that curve away from the polar axis resulting in defective sutures.<sup>27</sup> Homozygous AQP0 knockout (KO) mouse lenses completely fail to form sutures.<sup>27</sup>

Here we describe the phenotypes of functional genetic knockouts of *aqp0a* and/or *aqp0b* in zebrafish. Genetic mutants overcome the limitations of MO knock-down experiments, which can have off-target effects and are only effective at embryonic and early larval stages. The presence of embryonic cataracts in mutants confirms our original MO results that both *Aqp0a* and *Aqp0b* play essential roles in early lens development. While the lenses of single mutants show variably penetrant cataracts with distinct cellular phenotypes, double mutants show highly penetrant, severe cataracts, supporting the conjecture that *Aqp0a* and *Aqp0b* have both unique and partially redundant functions.

Large adult *aqp0a*<sup>-/-</sup>, but not *aqp0b*<sup>-/-</sup>, mutant lenses develop anterior polar opacification, accompanied by anterior sutural instability, disorganization of fiber cell architecture, and a mass of nuclei at the anterior pole. We also found, unexpectedly, that normal development of zebrafish lens optics relies on movement of the lens nucleus from an initial location near the anterior pole in juveniles to the center of the lens in adults. This shift requires *Aqp0a*. We propose that the instability of the anterior lens suture when *Aqp0a* is absent leads to failure of nuclear centralization, completely disrupting optics in adult lenses.

## METHODS

### Zebrafish Husbandry

The animal protocols used in this study adhered to the ARVO Statement for the Use of Animals in Ophthalmic and Vision Research. Zebrafish (AB strain) were raised and maintained under standard laboratory conditions.<sup>28</sup> Embryos used for lens transparency analysis were raised in 0.003% 1-phenyl-2-thiourea (PTU; Sigma-Aldrich Corp., St. Louis, MO, USA) to prevent pigment formation, and anesthetized in tricaine (MS-222; Sigma-Aldrich Corp.).

### Gene Manipulation

CRISPR/Cas9-mediated gene editing was used to create deletions in exon 1 of *Danio rerio* aquaporin 0a (*aqp0a*), also known as major intrinsic protein of lens fiber a (*mipa*; Gene ID 445140), or exon 1 of *Danio rerio* aquaporin 0b (*aqp0b*), also known as major intrinsic protein of lens fiber b (*mipb*; Gene

ID 553420). *Cas9* mRNA was injected along with a guide RNA (gRNA) designed using the online tool Chop Chop,<sup>29</sup> that targets either *aqp0a* (GGCACGAAACAGGGACATCT) or *aqp0b* (GGGGGCCATGGCAGGAGCCG). PCR genotyping (using primer pairs F: ACGAACACATAAATGGCACCT; R: TGGCCGATG GATTGGATGAA targeting *aqp0a* or F: TTTCGGCACCATGTTC TTCCG, R: GGCACGATGGCACTTAACAC targeting *aqp0b*) revealed out-of-frame deletions in the genomic DNA derived from sperm of male injected fish (F0s). These were outcrossed to generate heterozygous F1s, which were incrossed to generate homozygous F2 mutants. Single mutants of both genes were intercrossed to generate homozygous *aqp0a*<sup>-/-</sup>;*aqp0b*<sup>-/-</sup> double mutants. Homozygotes were crossed to generate maternal-zygotic homozygous mutants.

### Gross Lens Analysis and Lens Dissection

PTU-treated 2 to 4 dpf zebrafish were euthanized and lens transparency assessed using a microscope (Zeiss Axioplan 2; Oberkochen, Germany) with differential interference contrast (DIC) optics, which highlighted refractive abnormalities. Images were captured using a digital camera (ORCA-ER; Hamamatsu Photonics KK, Hamamatsu City, Japan) and acquired using commercial software (Velocity 5, version 5.2.1; PerkinElmer, Akron, OH, USA). Larval or adult zebrafish were euthanized and transparency of dissected lenses was visualized with a microscope and digital camera with a dynamic positioning controller (Olympus SZX12 microscope and Olympus DP70 with a model 2.1.1.183 controller; Olympus Corp., Tokyo, Japan). For in situ transparency assessment, a fiber optic light source (Schott KL 1500; Schott AG, Mainz, Germany) was used for oblique illumination from two sides to visualize opacities. Standard length and eye diameter were measured following previously established guidelines.<sup>30</sup> Lenses were dissected in phosphate buffered saline (PBS) (Fisher BioReagents, Pittsburgh, PA, USA) at room temperature (RT) and images were used to assess transparency under darkfield and brightfield illumination. Optical properties were assessed by the ability of lenses to focus a field finder grid (Lovins Field Finder; Electron Microscopy Sciences, Hatfield, PA, USA). Lenses were oriented equatorially, with poles and sutures perpendicular to the plane of focus, or axially, with poles and sutures parallel to the plane of focus. Zebrafish lenses are not completely rotationally symmetrical, so to determine lens size, diameters were measured in an equatorial orientation. The position of the lens nucleus center was normalized to lens size by expressing the position of the nucleus as the normalized coordinate,  $r/a$ , where  $a$  is the radius of the lens and  $r$  is the distance from the center of the lens to the center of the nucleus. The value of  $(a - r)$  is the distance of the center of the nucleus from the anterior pole, which is the number we actually measured, since it is difficult to precisely locate the center of the lens. We calculated the value of  $r/a$  as  $[1 - (a - r)/a]$ , where  $a$  and  $(a - r)$  were the actual measured values, for experimental convenience. For a nucleus at the center of the lens ( $r = 0$ ), the value of the normalized coordinate  $r/a$  is 0. For a nucleus centered at the surface of the lens (possible only for a point nucleus) the value of the normalized coordinate  $r/a$  is 1. In fact, we never observed a nucleus center closer to the surface than an  $r/a$  value of about 0.5.  $r/a$  was graphed as a function of standard length (SL). The positions of centers of adult nuclei were measured when the presumptive embryonic nucleus was evident.

### Lens Tissue Processing

Adult lenses were fixed in 1.5% (wt/vol) paraformaldehyde (PFA) (Electron Microscopy Sciences) in PBS for 24 hours at RT, while whole embryos were fixed whole in 4% PFA at 4°C

overnight. After PBS washes, embryos or lenses were cryoprotected by placing into 10% sucrose (wt/vol), 20% sucrose for 1 hour at RT and overnight in 30% sucrose at 4°C. We collected 12 to 14  $\mu\text{m}$  cryosections containing the lens onto gelatin-coated slides. Adult equatorial lens sections at 12 to 14  $\mu\text{m}$  were collected onto microscope slides (Superfrost/Plus; Fisher Scientific, Hampton, NH, USA). For whole lens analysis, after fixation, lenses were permeabilized in PBS + 10% Triton + 1% dimethyl sulfoxide (DMSO) overnight at 4°C. Lens membrane protein was extracted from decapsulated adult zebrafish lenses (ProteoExtract Native Membrane; Calbiochem, La Jolla, CA, USA).

### Antibodies

Polyclonal rabbit anti-sera were raised against C-terminal peptides of zebrafish Aqp0a (CVRGLSERLAVLKGNK) or Aqp0b (CFSERLATLKGSRPPE; Covance, Inc., Princeton, NJ, USA) as per Froger et al.,<sup>17</sup> and purified (Econo-Pac Serum IgG; Bio-Rad Laboratories, Hercules, CA, USA). Aqp0a and Aqp0b peptides for competition studies were also generated (Thermo Fisher Scientific, Rockford, IL, USA). Monoclonal mouse anti-alpha Tubulin (GT114) was purchased from Genetex (Irvine, CA, USA).

### Immunohistochemistry

Embryonic head sections or adult lens sections were labeled with anti-Aqp0a or anti-Aqp0b antibodies (1:500) overnight at 4°C. Following PBS washes, AlexaFluor 488 goat anti-rabbit secondary antibody (1:500; Thermo Fisher Scientific) was applied for 2 hours at RT. Lens plasma membranes were labeled with wheat germ agglutinin AlexaFluor 594 (1:50; Life Technologies, Grand Island, NY, USA) and DAPI (1:1000) for 2 hours at RT or overnight at 4°C. Whole permeabilized lenses were incubated in AlexaFluor Phalloidin-546 (1:200; Thermo Fisher Scientific) and DAPI (1:1000). Images were acquired with a confocal microscope and imaging software (Nikon Eclipse Ti-E with NIS-Elements AR; Nikon Corp., Tokyo, Japan). Images were viewed and compiled using a commercial viewer (NIS-Elements, version 4.2; Nikon Instruments, Melville, NY, USA) and ImageJ, version 1.51n (<http://imagej.nih.gov/ij/>; provided in the public domain by the National Institutes of Health, Bethesda, MD, USA) and a raster graphics editor (Adobe Photoshop CS5, version 12.0; Adobe Systems, San Jose, CA, USA).

### Western Blot Analysis

Proteins were separated by SDS-PAGE and transferred onto nitrocellulose membranes. Proteins were labeled by incubation with rabbit anti-Aqp0a or anti-Aqp0b antibodies (1:500) overnight at 4°C, and goat anti-rabbit horse radish peroxidase (HRP) (1858415, 1:10,000; Pierce Biotechnology, Waltham, MA, USA) for 1 hour at RT and visualized by ECL Prime (GE Healthcare Life Sciences, Pittsburgh, PA, USA) using the Fujifilm LAS 4000 imager (Tokyo, Japan). To ensure equal protein loading, blots were stripped (2% SDS, 0.7%  $\beta$ -mercaptoethanol, 0.775% Tris-HCl [wt/vol] in TBS-T) for 30 minutes at 50°C, blocked, and incubated with mouse anti-alpha Tubulin (1:500) overnight at 4°C, followed by goat anti-mouse HRP (1858413, 1:8000; Pierce Biotechnology) for 1 hour at RT and visualized as above.

### Statistical Analysis

R commander version 3.3.0 (from 2016-05-03) was used for statistical analysis.<sup>31</sup> Standard linear regression was used to

assess the relationships between lens diameter and SL, eye diameter and SL, and lens diameter and eye diameter. A statistical test of proportions was used to estimate the difference in incidence rate of cataracts between each pair of genotype groups. The Holm method was used to calculate adjusted *P* values that account for multiple testing (six pairs of genotype groups necessitated six tests) of each data set (2, 3, and 4 dpf).<sup>32</sup> The log of the normalized axial nucleus measurement (*r/a*) had an approximately linear relationship with SL (Supplementary Fig. S3), so linear regression was used to assess the relationship between the log normalized axial nucleus measurement and SL, controlling for genotype group. All computations and graphics were completed in the statistical language and programming environment R.

## RESULTS

### Embryonic and Adult Lens Transparency Require Both Aqp0a and Aqp0b

To study the roles of Aqp0a or Aqp0b in lens development, transparency and function, we created loss-of-function *aqp0a*, *aqp0b*, and *aqp0a/b* mutants using CRISPR-Cas9-mediated gene editing (Fig. 1A). Loss of either Aqp0a or Aqp0b protein in mutants was confirmed by Western blot analysis (Fig. 1B). The effects of loss of Aqp0a and/or Aqp0b function on lens transparency were analyzed in living embryos using DIC imaging. At 2 to 3 dpf, lenses in a subset of embryos displayed obvious opacities, which became less evident by 4 dpf (Fig. 2A). Cataract frequency at 2 dpf was 8% in *aqp0a*<sup>-/-</sup>, 9% in *aqp0b*<sup>-/-</sup>, and 36% in double mutants, compared to 1% in WT (Fig. 2B) and by 3 dpf was ~12.5% in both single and double mutant fish (0% in WT; Supplementary Fig. S1). Morphologic defects were restricted to the lens nucleus at both 2 and 3 dpf, while the lens cortex and epithelium appeared unaffected (Fig. 2A). Unexpectedly, cataracts in double mutants typically appeared less severe than in single mutants (Fig. 2A, right column). While the obvious cataracts seen at earlier stages in the mutants disappeared by 4 dpf (Figs. 2A, 2B), refractive defects remained. These manifested as marked differences in refraction at the cortex-nucleus interface in contrast to the consistently clear, smoother refractive gradient at the cortex-nucleus boundary of WT lenses (Fig. 2A arrows, bottom row).

Transparency in anesthetized older fish lenses was analyzed in vivo using an oblique light to highlight opacity under brightfield illumination (Figs. 3A, 3B). To localize regions of lens opacity in mutants, dissected adult lens transparency was assessed by darkfield illumination at both poles, as well as the nuclear and equatorial regions (Fig. 3C). In juvenile fish at 16 to 18 mm SL, only double mutant lenses showed obvious opacity (Fig. 3A). In adults larger than 23 mm SL, *aqp0a*<sup>-/-</sup> mutants also exhibited opacity (Fig. 3B) localized to the anterior pole (Fig. 3C; anterior pole is outlined with a dotted line). This was not evident in *aqp0b*<sup>-/-</sup> mutants (Figs. 3B, 3C). Double mutant lenses had similar anterior polar opacities as well as obvious nuclear cataracts (Fig. 3C). Although the severity and extent of the opacity from the center of double mutant lenses varied (Supplementary Fig. S2), cataracts were consistently present in embryonic nuclei, which are comprised of primary fiber cells.<sup>33</sup>

To analyze the consequences of the opacity observed in vivo on lens transparency and optics, adult dissected lenses were imaged through their optical axis (equatorial orientation). Both brightfield and darkfield illumination revealed mild refractive problems in *aqp0a*<sup>-/-</sup> mutants at the cortex-nucleus interface and at the lens periphery. But with the same illumination, double mutants showed obvious nuclear opacity

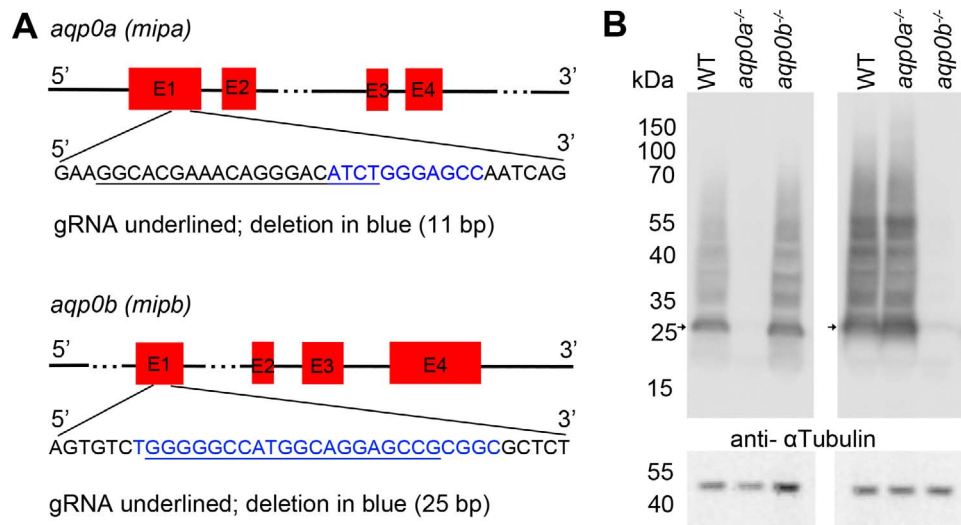


**FIGURE 1.** CRISPR-Cas9 mediated Aqp0a or Aqp0b functional knock-out. (A) gRNA designed against exon 1 of *aqp0a* or *aqp0b* co-injected with Cas9 resulted in out-of-frame deletions (11 bp for *aqp0a* and 25 bp for *aqp0b*) that are predicted to create premature stop codons. Mutants identified by PCR were confirmed by DNA sequencing. (B) Maternal-zygotic mutant adult lens fiber membrane protein was run on a Western blot. (B, top) Failure to detect at the monomeric molecular weight of ~28 kDa (arrow), as well as labeling of the polymeric bands was observed in *aqp0a*<sup>-/-</sup> by anti-Aqp0a antibody, and *aqp0b*<sup>-/-</sup> by anti-Aqp0b antibody, while the other ortholog was still detected. Stripping and reprobing the blot with anti- $\alpha$ -Tubulin antibody (B, bottom) served as a protein loading control.

and more widespread cortical fiber-to-fiber membrane stacking defects (for more examples of double mutant phenotypes, see Figs. 4A, 4B, Supplementary Fig. S2).

The ability of lenses to focus a grid image provided a rough assessment of their optical properties. Grids behind WT and *aqp0b*<sup>-/-</sup> mutant lenses were visible and well-focused (Fig. 4C). But grids behind *aqp0a*<sup>-/-</sup> and double mutant lenses were almost invisible and blurred (Fig. 4C).

To determine Aqp0 effects on growth, lens size was compared with eye size and standard length (SL) in *aqp0a*<sup>-/-</sup>, *aqp0b*<sup>-/-</sup>, and *aqp0a/b* mutants using brightfield imaging. As zebrafish grow at different rates depending on food availability, anterior eye segment size correlates better with SL than with age,<sup>34</sup> so SL was used for staging past 4 dpf.<sup>30</sup> Lenses in the double mutants grew slower than in WT or single mutants, and this was lens-specific, not a result of delayed eye growth (Supplementary Figs. S3, S4). Thus, in addition to their roles in lens transparency, Aqp0a and Aqp0b have partially redundant roles in lens growth.

### Aqp0a and Aqp0b Show Similar Spatial and Temporal Expression Patterns

Phenotypic differences between *aqp0a*<sup>-/-</sup> and *aqp0b*<sup>-/-</sup> mutants could reflect spatially and temporally specific patterns of protein expression. To test this, Aqp0a and Aqp0b expression was examined by immunohistochemistry in sections. Purified antibodies directed against the C-termini of Aqp0a or Aqp0b detected a punctate signal for both at 1 dpf (Figs. 5A, 5B, green). At 2 dpf, the labeling strongly correlated with lens cell membranes (WGA, red), and became restricted to the cortical fiber cell membranes from 3 dpf onward. Antibodies were also tested on mutant lenses, confirming specificity for each ortholog (Figs. 5C, 5D). As is well documented in mammalian lens fiber cells,<sup>35</sup> C-terminal immunoreactivity of Aqp0a and Aqp0b was lost in mature lens fiber cells. This coincided with degradation of nuclei (blue) in the lens center, as well as loss of WGA signal,

indicating the tight compaction of fiber cells to form the lens nucleus.

Anti-Aqp0a (Fig. 5E) or anti-Aqp0b (Fig. 5F) antibodies strongly labeled all cortical fiber cell membranes in adult zebrafish lenses. Immunoreactivity was abruptly lost at the boundary between the inner cortex and lens nucleus, where it was completely absent. The normalized fluorescence intensity of Aqp0a and Aqp0b as a function of normalized distance from the lens center (0.0 is the lens center, and 1.0 is the epithelium) showed that the C-terminal signals for both, Aqp0a and Aqp0b, was lost at an  $r/a$  of about 0.65. Thus, Aqp0a and Aqp0b show very similar patterns of when they are first detected, how they insert into the membrane, and how they localize to the periphery.

### Aqp0a Is Required for Nuclear Centralization and Anterior Suture Stability

To probe the mechanisms leading to the anterior polar opacification seen in *aqp0a*<sup>-/-</sup> mutants but not in *aqp0b*<sup>-/-</sup> mutants, lenses were dissected at four developmental stages and imaged perpendicular to the optical axis (axial orientation; Fig. 6A). Surprisingly, in young WT lenses (3.4–3.7 mm SL) the lens nucleus was initially displaced toward the anterior pole ( $r/a \sim 0.2$ ) and later centralized in full-grown adults ( $r/a = 0.0$ ; Fig. 6B). *aqp0a*<sup>-/-</sup> and double mutant lens nuclei also started off closer to the anterior pole in young fish; but in *aqp0a*<sup>-/-</sup> adult mutant lenses, the nucleus failed to centralize and remained shifted toward the anterior even in older fish ( $r/a \sim 0.1$  at 25 mm SL). In double mutants, nuclear centralization was completely disrupted, and nuclear position varied greatly, with a mean estimated axial nucleus center location of  $r/a \sim 0.2$  at all stages (Figs. 6A, 6B; Supplementary Figure S5).

Anterior polar opacification and anterior displacement of the lens nucleus could result, at least in part, from defects in the stability of the anterior suture. To assess suture integrity, whole fixed lenses were examined for fiber cell morphology using F-actin immunohistochemistry and cell nuclear position using DAPI staining (Fig. 7). Z-projections of the anterior pole

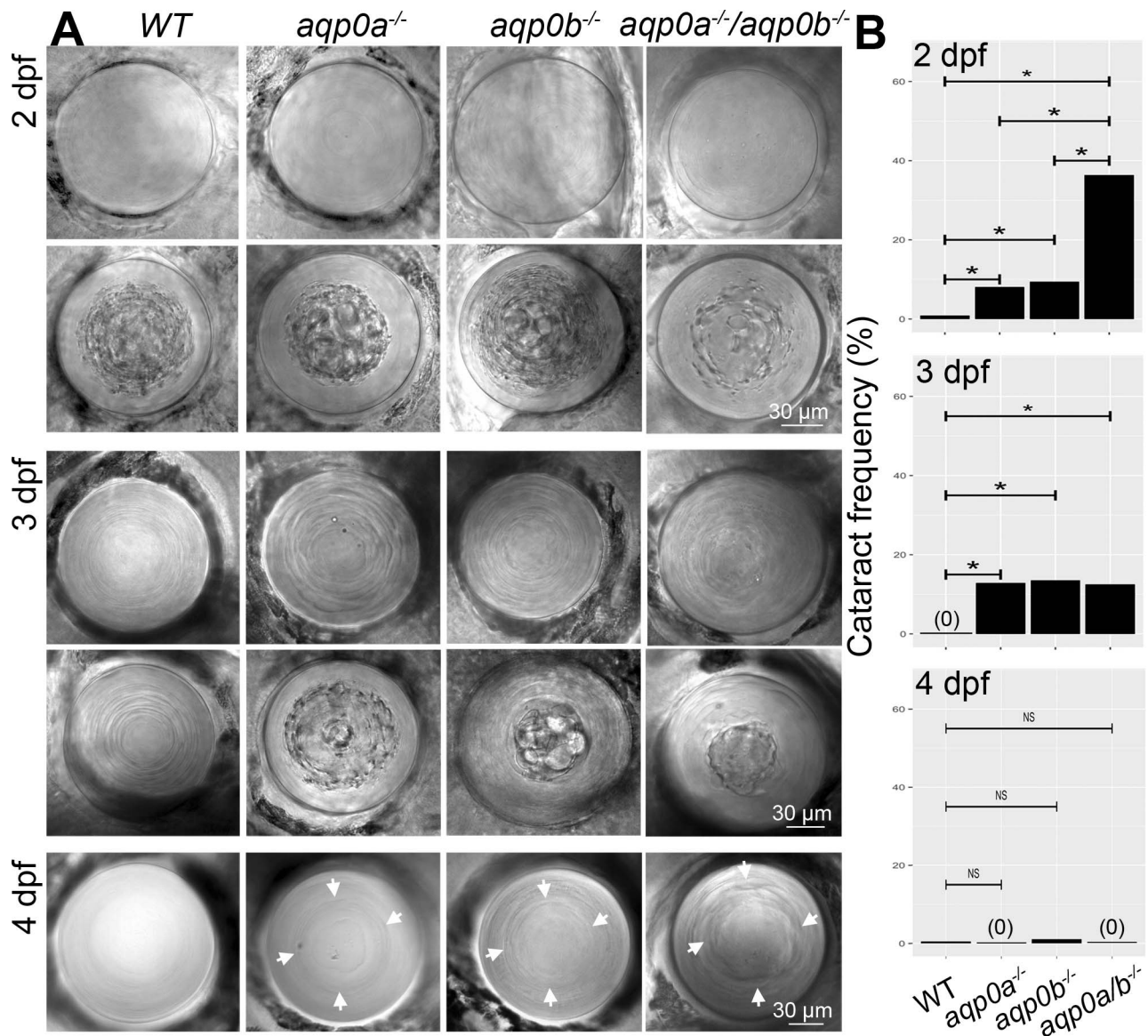


**FIGURE 2.** Loss of Aqp0a and/or Aqp0b increases frequency of embryonic cataract. (A) Representative in vivo DIC images of clear and cataractous lenses from WT, *aqp0a*<sup>-/-</sup>, *aqp0b*<sup>-/-</sup> or double mutant embryos taken at 2, 3, and 4 dpf. Refractive defects at the cortex-nucleus interface at 4 dpf are indicated by white arrows. (B) Cataract frequency was quantified at 2, 3, and 4 dpf by binary readout. A statistical test of proportions was used to estimate the difference in incidence rate of cataracts between each pair of genotype groups. The Holm method was used to calculate adjusted *P* values that account for multiple testing. Statistically significant differences at 95% confidence are indicated by an asterisk. See Supplementary Figure S1 for full statistical analyses.

(Fig. 7A) as well as analysis of optical slices taken 46  $\mu$ m from the anterior pole (Fig. 7B) revealed that while WT and *aqp0b*<sup>-/-</sup> fiber cell morphology was highly ordered, with fiber cell rows meeting in the center to form the anterior suture, *aqp0a*<sup>-/-</sup> and double mutant anterior poles displayed a disorganized mass of F-actin labeling as well as ectopic fiber cell nuclei often occupying the position of the anterior suture (Figs. 7A, 7B). Furthermore, deeper in the lens cortex, 76  $\mu$ m from the anterior pole where WT lenses had no nuclei in the fiber cells, *aqp0a*<sup>-/-</sup> and double mutants had many ectopic fiber cell nuclei, while *aqp0b*<sup>-/-</sup> mutants also showed the occasional ectopic fiber-cell nucleus (Fig. 7C). Though anterior sutures were disrupted to a greater or lesser extent in all *aqp0a*<sup>-/-</sup> or double mutants, posterior sutures were intact in all genotypes and were devoid of nuclei (Fig. 7D). Thus, cataracts and nuclear displacement in Aqp0-deficient lenses correlated with disruption of the anterior suture.

## DISCUSSION

Water transport, adhesion, and cytoskeletal protein anchoring are essential functions provided by AQP0 that ultimately determine lens physiology and optics. It has been impossible to determine how each individual function contributes to lens transparency in mammalian systems, but such a distinction is facilitated in zebrafish by subfunctionalization of duplicate Aqp0s in teleosts.<sup>17,18</sup> Here we show by functional knock out of the two zebrafish AQP0 orthologs that Aqp0a, but not Aqp0b, is required for anterior suture stability, consistent with a role for water transport at the suture. By analyzing the time course of the appearance of these suture defects, we also discovered that the zebrafish lens nucleus shifts from an anterior position at younger stages, to a central location in the adult lens and that this shift fails in Aqp0a mutants. We propose that this early lens

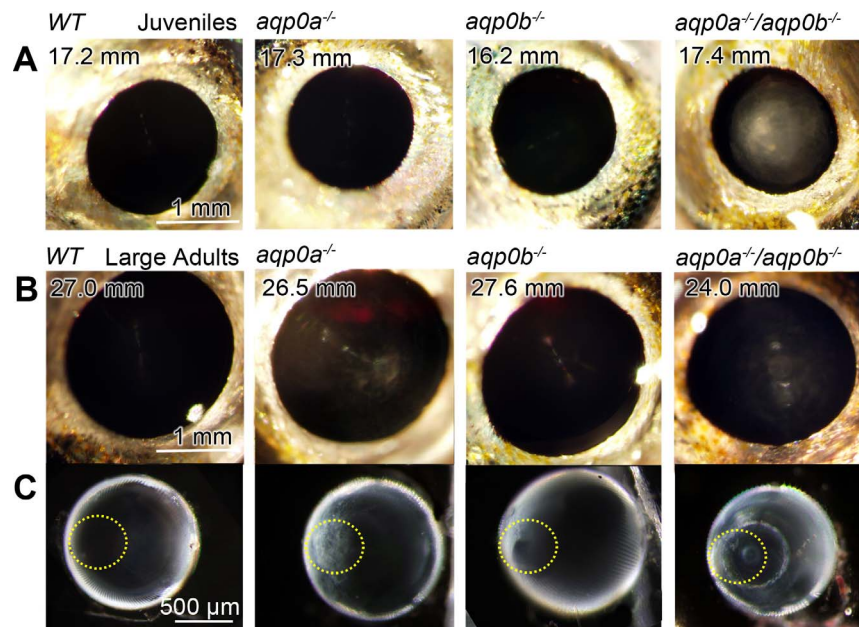


**FIGURE 3.** Cataracts form in double mutants and large *aqp0a*<sup>-/-</sup> mutants. Lens opacity assays were performed on live, anesthetized fish at a range of juvenile and adult stages. WT fish had no cataracts at any stage analyzed, even at very large adult stages. Double mutants had cataracts at all stages analyzed: (A) SL 8 to 11 mm (100%, *n* = 4 fish), 11 to 15 mm (100%, *n* = 6), 15 to 20 mm (100%, *n* = 11); (B) 20 to 23 mm (100%, *n* = 2), > 23 mm (100%, *n* = 3). At young stages, *aqp0a*<sup>-/-</sup> or *aqp0b*<sup>-/-</sup> mutants had no opacity (A) shown at 15–20 mm SL, while large adult *aqp0a*<sup>-/-</sup> (> 23 mm) had consistent cataract (100%, *n* = 8) compared to much lower frequency in *aqp0b*<sup>-/-</sup> (25%, *n* = 8, lenses were typically clear as shown in [B]). Excised lenses from *aqp0a*<sup>-/-</sup> or double mutant large adults had anterior polar opacities (anterior pole is outlined with a yellow dotted line) while double mutants also had nuclear cataracts (C). Please see Supplementary Figure S2 for more examples of double mutant phenotypes.

placement anteriorly is required for emmetropia at larval stages and its centralization depends on a stable anterior suture (Fig. 8). These results further support our previous evidence for overlapping but distinct functions for Aqp0a and Aqp0b in the lens and set the stage for future experiments testing the ability of mutant constructs lacking

water transport, cytoskeletal regulation, or adhesion to rescue mutant phenotypes to test these hypotheses.

### Overlapping Roles for Aqp0a and Aqp0b

A lens still forms in *aqp0a/b* double mutants, indicating that Aqp0 function is not required for lens specification or

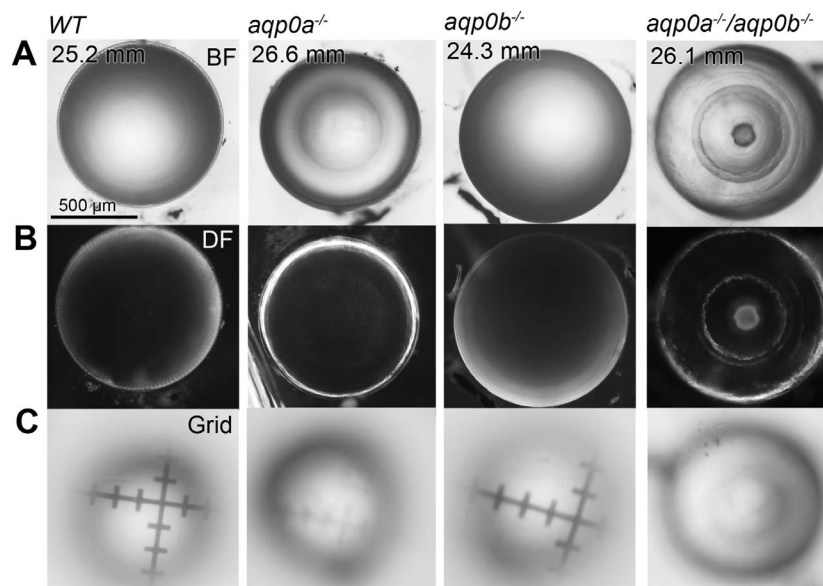


**FIGURE 4.** Aqp0a is required for normal lens optics. Representative lenses dissected from WT, *aqp0a*<sup>-/-</sup>, *aqp0b*<sup>-/-</sup>, or double mutant zebrafish of SL > 23 mm imaged through their optical axis (equatorial orientation). Lenses imaged under brightfield (BF; [A]) and darkfield (DF; [B]) illumination reveal a clear lens for WT and *aqp0b*<sup>-/-</sup> mutants, while *aqp0a*<sup>-/-</sup> mutants have mild refractive changes between the nucleus and lens periphery. Double mutant lenses have a severe nuclear cataract with cortical refractive problems. (C) Optical properties of lenses were tested by focusing through the lens onto micrometer grids, which revealed poor optical properties of the *aqp0a*<sup>-/-</sup> and double mutant lenses.

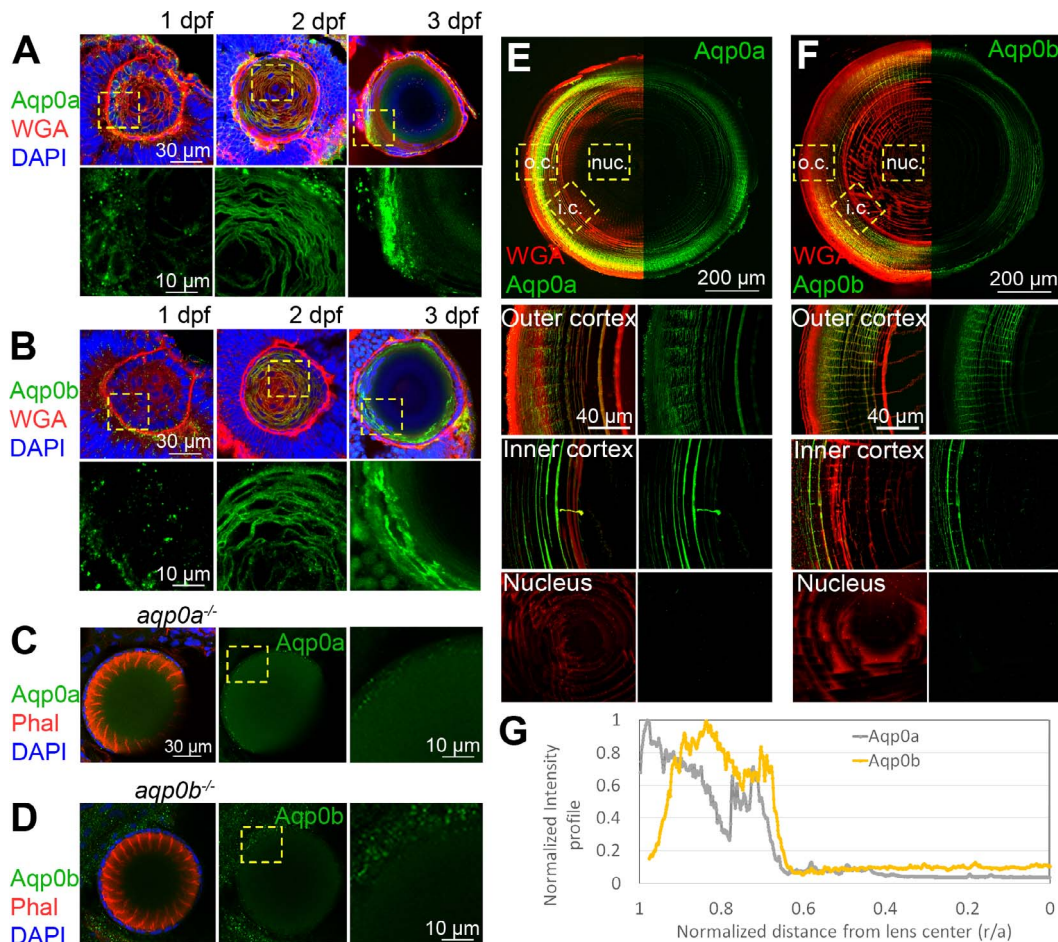


**FIGURE 5.** Expression of Aqp0a and Aqp0b in WT zebrafish lenses; 1 to 3 dpf eye cryosections labeled with (A) anti-Aqp0a or (B) anti-Aqp0b antibodies (green), plasma membrane label wheat germ agglutinin (WGA, red), and DAPI (blue). High power images of Aqp0a or Aqp0b labeling only were taken from regions outlined by yellow-dashed boxes. *aqp0a*<sup>-/-</sup> lenses labeled for F-actin (phalloidin, red) and DAPI (blue) as well as with (C) anti-Aqp0a antibody, and *aqp0b*<sup>-/-</sup> labeled with (D) anti-Aqp0b antibody serve as negative controls. Adult lens cryosections were labeled with (E) anti-Aqp0a or (F) anti-Aqp0b antibodies (green), and WGA (red). Equatorial lens section is shown with antibody labeling only detected in the cortex. High power images from the outer cortex (o.c.), inner cortex (i.c.), and nucleus (nuc.) are taken from regions outlined by yellow dashed boxes. (G) Normalized intensity of either Aqp0a (gray) or Aqp0b (yellow) antibody labeling in adult lenses as a function of distance from lens center. Each experiment is representative of at least six independent lenses analyzed.

differentiation. However, double mutant lenses grow slower and severe morphologic and optic defects arise earlier than in single-mutant lenses, providing evidence for at least some functional redundancy between the two orthologs, including a conserved role in lens growth. Similarly, mouse lenses lacking AQP0 function have reduced lens diameters and wet weight.<sup>36–38</sup> Taken together, the zebrafish and mouse results suggest that Aqp0a and Aqp0b share a common lens development property with mammalian AQP0, possibly water permeability. Reduced size could be a result of decreased water transport into the lens via Aqp0, which in mice accounts for 80% of water permeability of lens fiber cell membranes.<sup>36</sup> Thus, mammalian and zebrafish Aqp0s have conserved roles in lens development, likely due to their functions in water permeability.

*aqp0a/b* double mutants also form cataracts at a higher frequency at 2 dpf than either single mutant (Fig. 2A), suggesting an additive effect of losing both Aqp0s on a common water transport function. Cataracts persist at 3 dpf, when the zebrafish lens nucleus compacts and loses both fiber cell nuclei and organelles (Fig. 5A), and likely becomes emmetropic in WT.<sup>59</sup> Strikingly, however, obvious cataracts

are no longer visible at 4 dpf in single or double mutants (Fig. 2A). Cataracts induced by morpholino knockdown of *aqp0* expression also recover lens transparency at similar stages,<sup>17,18</sup> but this recovery was attributed to a gradual loss of morpholino effectiveness. The present results suggest instead that the lens can compensate for the loss of Aqp0 function, at least temporarily, to restore transparency. We speculate that early embryonic cataracts in zebrafish likely reflect transient loss of cell volume regulation—either cell swelling or accumulation of extracellular fluid between fiber cells. In the absence of either or both Aqp0 proteins, this volume disruption is corrected at 4 dpf, likely by another osmoregulatory mechanism. AQP5, the other AQP present in mammalian lenses<sup>35,40</sup> would be a logical osmoregulatory candidate. Zebrafish, however, lack a clear AQP5 homolog,<sup>41</sup> which has been suggested to have arisen as a terrestrial adaptation associated with hydration of the cornea and nictitating membrane (see Ref. 42 for review).

We observed a lower frequency of cataracts at 3 dpf (~12%) for all mutants compared to previous MO knockdowns of either Aqp0 (~80%).<sup>18</sup> This could reflect differences in genetic compensation, off-target effects,<sup>45</sup> or MO toxicity and upreg-



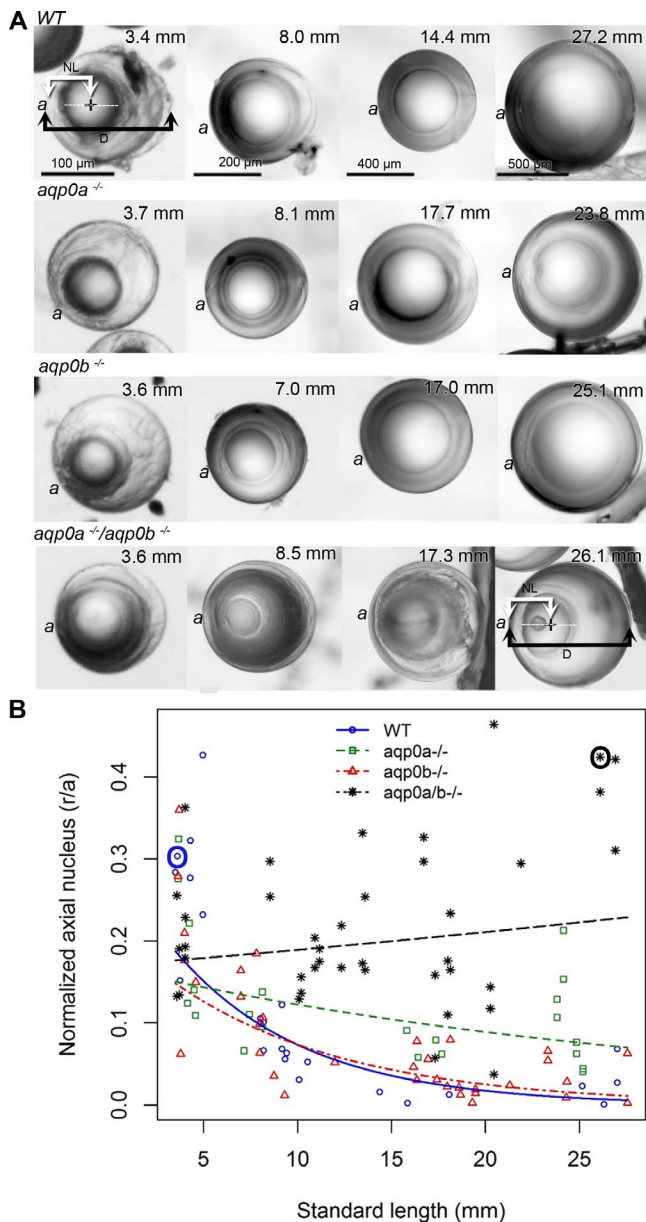


**FIGURE 6.** Aqp0a is required for lens nucleus centralization. (A) Lens sutures were used to orient lenses perpendicular to the optical axis (axial orientation). The anterior lens pole (*a*) is indicated (please note that although fish have laterally facing eyes, in this manuscript we are using “anterior” as the part of the lens that sees light first). Representative lenses are shown from fish of indicated SL. Measurements were taken as shown in WT at 3.4 mm SL and double mutants at 26.1 mm SL, and resulting data points circled (in blue for WT, and black for double mutants in [B]). The distance from the center of the nucleus (*plus*) to the anterior pole (NL) was expressed as a ratio of lens radius (*D/2*). (B) The normalized distance of the center of lens nucleus to the anterior pole (*r/a*), where 1.0 is the lens surface, and 0.0 is the center of the lens, is graphed as a function of SL. Linear regression fits were used to assess the relationship between log normalized axial nucleus localization and SL. The estimated regression slope of *aqp0a*<sup>-/-</sup> was significantly different from WT ( $P = 9.85\text{e-}05$ ) and *aqp0b*<sup>-/-</sup> ( $P = 0.00388$ ). The estimated regression slope of double mutants was significantly different from WT ( $P = 7.55\text{e-}08$ ) and *aqp0b*<sup>-/-</sup> ( $P = 5.21\text{e-}06$ ). See Supplementary Figure S5 for full statistical analyses.

ulation of p53,<sup>44</sup> which can cause stress-induced defects in lens morphology.<sup>45,46</sup> Rescue of MO-induced cataracts by injection of DNA constructs encoding Aqp0<sup>18</sup> supports genetic specificity of the knockdowns.

Despite the lack of obvious cataracts at 4 dpf, *aqp0a/b* double mutant lenses, and to a lesser extent the single mutants, show refractive problems at this stage. This is characteristic of fiber stacking defects (Fig. 2A), similar to that seen in *fn*<sup>-/-</sup> zebrafish lenses.<sup>26</sup> An oblique light-source reveals that nuclear cataracts reappear in double mutants beginning at 6 dpf (Supplementary Fig. S2A). In contrast, nuclear cataracts do not form or reappear in single mutants (Figs. 3, 4, 6). Our results suggest overlapping functions for Aqp0a and Aqp0b in early lens development, specifically for stacking and maintenance of the embryonic lens nucleus.

Based on our immunohistochemical analyses, it seems unlikely that the distinct phenotypes of *aqp0a*<sup>-/-</sup> and *aqp0b*<sup>-/-</sup> are due to spatial, temporal, or subcellular differences in Aqp0a and Aqp0b protein expression and localization. Furthermore, both show C-terminal signal loss in mature fiber cells. This could be due to inaccessibility of the epitope due to the compaction of fiber cells, but more likely results from proteolytic cleavage and is well-documented for AQP0 in mammalian fiber cells as they age. However, this appears to occur closer to the lens periphery in zebrafish ( $r/a = 0.65$ ) than in rat ( $r/a = 0.35$ ),<sup>47</sup> and this shift may account for the higher refractive index of the zebrafish lens (1.41–1.55) compared to those of rodent lenses (1.38–1.48 in mouse).<sup>48</sup> Therefore, the difference between phenotypes must lie in the 15% difference in amino acid identity between the fish and mammalian AQP0s.<sup>17</sup>

### A Novel Role for Aqp0 in Lens Nucleus Centralization

Zebrafish lens development at embryonic and early larval stages, as well as in adults, has previously been well described in the literature.<sup>34,39,49</sup> However, developmental changes in the lens between 6 dpf and adulthood have not been systematically documented. We discovered that the lens nucleus first forms at the anterior pole and progressively centralizes with age, a phenomenon not described in the lenses of other species. Centralization requires Aqp0a, but not Aqp0b, confirming subfunctionalization between the two orthologs.

What is the functional significance of this nuclear displacement? Larval zebrafish rely on vision for hunting and evading predators as early as 5 to 6 dpf. Due to the short lens-to-retina distance at these early stages, we propose that positioning the high-refractive-index lens nucleus closer to the anterior pole facilitates focusing light onto the retina for emmetropization (Fig. 8A). As the lens grows, the lens-to-retina distance increases, and a centrally located lens nucleus now provides a better focus.

This may indeed be a common feature of aquatic species, particularly those with free-swimming, feeding larvae that need to develop a functional visual system early in life. Interestingly, sea bream (*Acanthopagrus butcheri*), like zebrafish, rely on their vision for survival at early stages (from 3–5 dpf), and have different focal ratios (focal length: lens diameter) between the optical axis and temporal or nasal axes.<sup>50</sup> Shand and colleagues<sup>50</sup> suggest that these different focal ratios may compensate for a relatively high Matthiessen’s ratio (distance of center of the lens to the retina: lens radius) in small eyes early in development. Our results argue that the anterior shift of the lens nucleus along the optical axis improves the visual acuity of very young fish with short lens-to-retina distances.

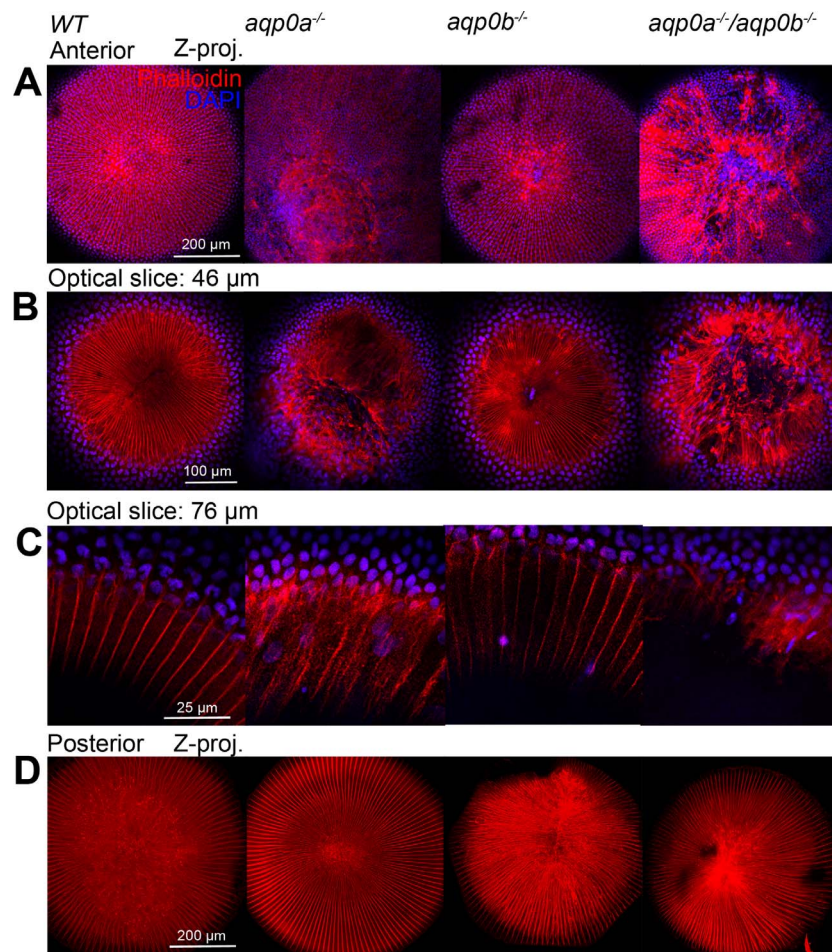


**FIGURE 7.** Aqp0a is required for anterior suture stability. Fixed and permeabilized large adult zebrafish lenses were labeled for F-Actin with phalloidin (red) and nuclei with DAPI (blue). Maximum z-projections were generated from 150 μm z-stacks of the anterior pole (A) and 150 μm z-stacks of the posterior pole (D) revealing the anterior, and posterior sutures, respectively. Optical slices 46 μm from the anterior pole reveal detail of the anterior sutures, which are severely damaged in *aqp0a*<sup>-/-</sup> and double mutant lenses (B). High power images of peripheral fiber cells and epithelial cells from an optical slice taken 76 μm from the anterior pole reveal the presence of nuclei in fiber cells in mutant lenses compared to WT (C). The cell nuclei within fiber cells counted in the whole optical slice taken 76 μm for WT: 0, *aqp0a*<sup>-/-</sup>: 38, *aqp0b*<sup>-/-</sup>: 2, double mutants: 21.

### Aqp0a Regulates Anterior Suture Stability

Anterior polar opacity and failure of the lens nucleus to centralize in *aqp0a*<sup>-/-</sup> mutants correlates with a defect in anterior pole integrity as assessed by F-actin immunohistochemistry. *aqp0a*<sup>-/-</sup> and double mutants exhibit epithelial and fiber cell disruptions that extend into the anterior cortex, while the *aqp0b*<sup>-/-</sup> lens anterior pole is unaffected (Fig. 7). This correlates with reduced and disorganized F-actin labeling. Multilayered epithelial cell nuclei also appear to fuse with a mass of underlying fiber cell nuclei in place of the anterior suture. Since younger *aqp0a*<sup>-/-</sup> lenses do not display anterior polar opacity, or obvious sutural defects, these results suggest a defect in suture stability as the lens grows.

Why is an AQP0 so critical for anterior suture stability? This is a conserved feature of AQP0 since lens sutures fail to form in mouse AQP0<sup>-/-</sup> lenses,<sup>27</sup> and multilayered anterior epithelia result in anterior polar cataracts in Cat<sup>Fr</sup> homozygous lenses (AQP0 with a long tandem repeat sequence insertion).<sup>51,52</sup> Our previous studies suggest that in zebrafish, Aqp0a is primarily a water channel, unlike Aqp0b, suggesting that water transport may be particularly critical at the anterior suture. The rapid elongation of differentiating fiber cell tips is achieved by

increases in cytoplasmic volume. The anterior tips of fiber cells may rely on Aqp0a for this influx. Interestingly, swelling of the anterior tips of differentiating lens fiber cells has also been described in Cat<sup>Fr</sup> lenses,<sup>53</sup> hinting at similar dysregulation of water transport by Aqp0a at these tips. Future studies using lens vesicles derived from Aqp0 mutant zebrafish lenses will address this issue.

Sutural instability may arise by different mechanisms in fish and mice. In Cat<sup>Fr</sup> lenses, sutural disruptions are evident early (postnatal days 1–14),<sup>53</sup> whereas zebrafish lens anterior opacities and anterior pole disruptions only appear at adult stages. AQP0 may function as a cytoskeletal anchor shaping sutural structure. Mammalian AQP0 interacts with filensin,<sup>4</sup> and such a role is consistent with the defects we see in the actin filament cytoskeleton of *aqp0a*<sup>-/-</sup> lenses. Moreover, the actin cytoskeleton is central to lens development and transparency.<sup>54</sup> Future experiments testing the ability of injected mutant constructs that eliminate water transport, cytoskeletal regulation, or adhesion to rescue the phenotypes of *aqp0a*<sup>-/-</sup> and double mutants will allow us to test these hypotheses.

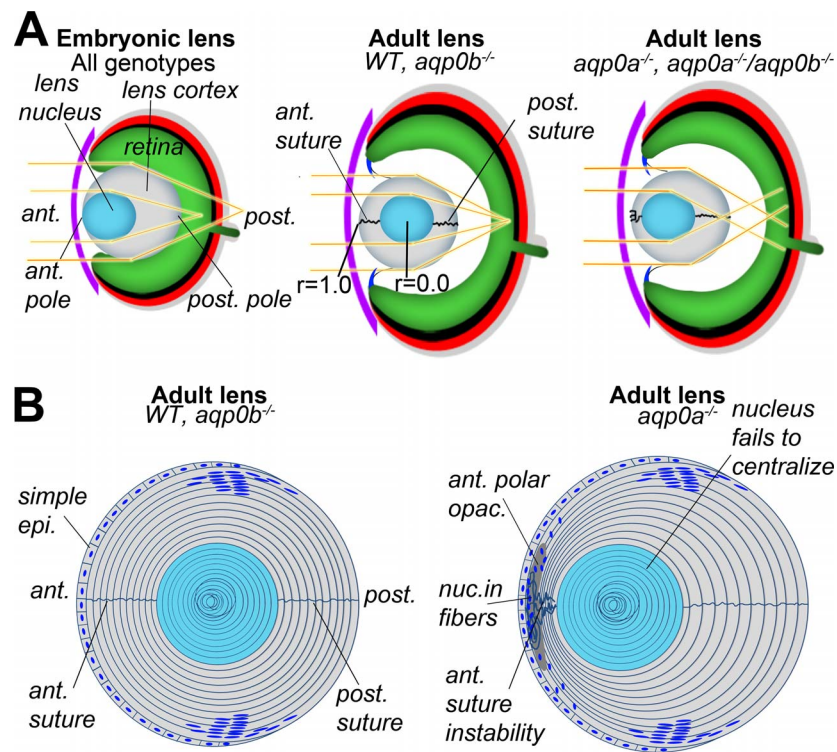


**FIGURE 8.** Development of zebrafish lens optics requires Aqp0a for anterior suture stability. (A) Lens nucleus localization at the anterior pole in young zebrafish allows light to be focused onto the retina even though it is in close proximity to the lens (A, left). As the fish and eye grow, the lens-to-retina distance increases. Thus for the lens to remain emmetropic, the higher refractive index nucleus must shift toward the lens center (A, middle). This mechanism is disrupted when Aqp0a is missing (in *aqp0a<sup>-/-</sup>* and double mutants) and the lens nucleus fails to centralize (A, right). (B) We propose that the nucleus fails to centralize due to loss of function of Aqp0a, which is required to stabilize the adult zebrafish anterior suture. Sutural instability in large adult stages is accompanied by an accumulation of nuclei anteriorly in cortical fiber cells, disorganization of fiber cell rows and eventually anterior polar opacification (B, right).

### Acknowledgments

The authors thank MyPhuong Tran for help in purifying the rabbit anti-Aqp0a and anti-Aqp0b antibodies and Megan Smith from the Center of Statistical Consulting for carrying out the statistical analyses.

Supported by National Institutes of Health Grant R01 EY05661 (JEH).

Disclosure: **I. Vorontsova**, None; **I. Gehring**, None; **J.E. Hall**, None; **T.F. Schilling**, None

### References

- Shiels A, Bennett TM, Hejtmancik JF. Cat-Map: putting cataract on the map. *Mol Vis*. 2010;16:2007-2015.
- Hall JE, Mathias RT. The aquaporin zero puzzle. *Biophys J*. 2014;107:10-15.
- Kumari SS, Varadaraj K. Intact AQP0 performs cell-to-cell adhesion. *Biochem Biophys Res Commun*. 2009;390:1034-1039.
- Lindsey Rose KM, Gourdie RG, Prescott AR, Quinlan RA, Crouch RK, Schey KL. The C terminus of lens aquaporin 0 interacts with the cytoskeletal proteins filensin and CP49. *Invest Ophthalmol Vis Sci*. 2006;47:1562-1570.
- Nakazawa Y, Oka M, Furuki K, Mitsuishi A, Nakashima E, Takehana M. The effect of the interaction between aquaporin 0 (AQP0) and the filensin tail region on AQP0 water permeability. *Mol Vis*. 2011;17:3191-3199.
- Yu XS, Jiang JX. Interaction of major intrinsic protein (aquaporin-0) with fiber connexins in lens development. *J Cell Sci*. 2004;117:871-880.
- Liu J, Xu J, Gu S, Nicholson BJ, Jiang JX. Aquaporin 0 enhances gap junction coupling via its cell adhesion function and interaction with connexin 50. *J Cell Sci*. 2011;124:198-206.
- Kumari SS, Varadaraj K. Aquaporin 0 plays a pivotal role in refractive index gradient development in mammalian eye lens to prevent spherical aberration. *Biochem Biophys Res Commun*. 2014;452:986-991.
- Németh-Cahalan KL, Kalman K, Hall JE. Molecular basis of pH and  $Ca^{2+}$  regulation of aquaporin water permeability. *J Gen Physiol*. 2004;123:573-580.
- Fields JB, Németh-Cahalan KL, Freitas JA, Vorontsova I, Hall JE, Tobias DJ. Calmodulin gates aquaporin 0 permeability through a positively charged cytoplasmic loop. *J Biol Chem*. 2017;292:185-195.
- Reichow SL, Clemens DM, Freitas JA, et al. Allosteric mechanism of water-channel gating by  $Ca^{2+}$ -calmodulin. *Nat Struct Mol Biol*. 2013;20:1085-1092.
- Kalman K, Németh-Cahalan KL, Froger A, Hall JE. Phosphorylation determines the calmodulin-mediated  $Ca^{2+}$  response and water permeability of AQP0. *J Biol Chem*. 2008;283:21278-21283.
- Ball LE, Little M, Nowak MW, Garland DL, Crouch RK, Schey KL. Water permeability of C-terminally truncated aquaporin 0 (AQP0 1-243) observed in the aging human lens. *Invest Ophthalmol Vis Sci*. 2003;44:4820-4828.
- Kumari SS, Gandhi J, Mustehsan MH, Eren S, Varadaraj K. Functional characterization of an AQP0 missense mutation, R33C, that causes dominant congenital lens cataract, reveals impaired cell-to-cell adhesion. *Exp Eye Res*. 2013;116:371-385.

15. Nakazawa Y, Oka M, Funakoshi-Tago M, Tamura H, Takehana M. The extracellular C-loop domain plays an important role in the cell adhesion function of aquaporin 0. *Curr Eye Res.* 2017;42:617-624.
16. Vihtelic TS, Fadool JM, Gao J, Thornton KA, Hyde DR, Wistow G. Expressed sequence tag analysis of zebrafish eye tissues for NEIBank. *Mol Vis.* 2005;11:1083-1100.
17. Froger A, Clemens D, Kalman K, Németh-Cahalan KL, Schilling TF, Hall JE. Two distinct aquaporin 0s required for development and transparency of the zebrafish lens. *Invest Ophthalmol Vis Sci.* 2010;51:6582-6592.
18. Clemens DM, Németh-Cahalan KL, Trinh L, Zhang T, Schilling TF, Hall JE. In vivo analysis of aquaporin 0 function in zebrafish: permeability regulation is required for lens transparency in vivo analysis of aquaporin. *Invest Ophthalmol Vis Sci.* 2013;54:5136-5143.
19. Chauvigné F, Zapater C, Stavang JA, Taranger GL, Cerdà J, Finn RN. The pH sensitivity of Aqp0 channels in tetraploid and diploid teleosts. *FASEB J.* 2015;29:2172-2184.
20. Greiling TMS, Clark JI. Early lens development in the zebrafish: a three-dimensional time-lapse analysis. *Dev Dyn.* 2009;238:2254-2265.
21. Cheng C, Nowak RB, Fowler VM. The lens actin filament cytoskeleton: diverse structures for complex functions. *Exp Eye Res.* 2017;156:58-71.
22. Kuszak JR. The development of lens sutures. *Prog Retin Eye Res.* 1995;14:567-591.
23. Sugiyama Y, Lovicu FJ, McAvoy JW. Planar cell polarity in the mammalian eye lens. *Organogenesis.* 2011;7:191-201.
24. Sugiyama Y, Shelley EJ, Yoder BK, et al. Nonessential role for cilia in coordinating precise alignment of lens fibres. *Mech Dev.* 2016;139:10-17.
25. Lu JY, Mohammed TA, Donohue ST, Al-Ghoul KJ. Distribution of basal membrane complex components in elongating lens fibers. *Mol Vis.* 2008;14:1187-1203.
26. Hayes JM, Hartsock A, Clark BS, Napier HRL, Link BA, Gross JM. Integrin  $\alpha 5$ /fibronectin1 and focal adhesion kinase are required for lens fiber morphogenesis in zebrafish. *Mol Biol Cell.* 2012;23:4725-4738.
27. Al-Ghoul KJ, Kirk T, Kuszak AJ, Zoltoski RK, Shiels A, Kuszak JR. Lens structure in MIP-deficient mice. *Anat Rec A Discov Mol Cell Evol Biol.* 2003;273A:714-730.
28. Westerfield M. *The Zebrafish Book: A Guide for the Laboratory Use of Zebrafish (Danio rerio)*. Eugene, OR: University of Oregon Press; 2000.
29. Montague TG, Cruz JM, Gagnon JA, Church GM, Valen E. CHOPCHOP: a CRISPR/Cas9 and TALEN web tool for genome editing. *Nucleic Acids Res.* 2014;42:W401-W407.
30. Schilling TF. The morphology of larval and adult zebrafish. In: Nusslein-Volhard C, Dahm R. *Zebrafish*. Oxford London, Oxford University Press. 2002;261:59-94.
31. Team RC. *R: A Language and Environment for Statistical Computing*. Vienna, Austria: R Foundation for Statistical Computing; 2016.
32. Holm S. A simple sequentially rejective multiple test procedure. *Scand J Stat.* 1979;6:65-70.
33. Dahm R, Schonhaler HB, Soehn AS, van Marle J, Vrensen GFJM. Development and adult morphology of the eye lens in the zebrafish. *Exp Eye Res.* 2007;85:74-89.
34. Soules K, Link B. Morphogenesis of the anterior segment in the zebrafish eye. *BMC Dev Biol.* 2005;5:12.
35. Petrova RS, Schey KL, Donaldson PJ, Grey AC. Spatial distributions of AQP5 and AQP0 in embryonic and postnatal mouse lens development. *Exp Eye Res.* 2015;132:124-135.
36. Shiels A, Bassnett S, Varadaraj K, et al. Optical dysfunction of the crystalline lens in aquaporin-0-deficient mice. *Physiol Genomics.* 2001;7:179-186.
37. Kalman K, Németh-Cahalan KL, Froger A, Hall JE. AQP0-LTR of the CatFr mouse alters water permeability and calcium regulation of wild type AQP0. *Biochim Biophys Acta.* 2006;1758:1094-1099.
38. Zhou Y, Bennett TM, Shiels A. Lens ER-stress response during cataract development in Mip-mutant mice. *Biochim Biophys Acta.* 2016;1862:1433-1442.
39. Fadool JM, Dowling JE. Zebrafish: a model system for the study of eye genetics. *Prog Retin Eye Res.* 2008;27:89-110.
40. Sindhu Kumari S, Varadaraj K. Aquaporin 5 knockout mouse lens develops hyperglycemic cataract. *Biochem Biophys Res Commun.* 2013;441:333-338.
41. Tingaud-Sequeira A, Calusinska M, Finn R, Chauvigne F, Lozano J, Cerdà J. The zebrafish genome encodes the largest vertebrate repertoire of functional aquaporins with dual paralogy and substrate specificities similar to mammals. *BMC Evol Biol.* 2010;10:38.
42. Finn RN, Chauvigné F, Hlidberg JB, Cutler CP, Cerdà J. The lineage-specific evolution of aquaporin gene clusters facilitated tetrapod terrestrial adaptation. *PLoS One.* 2014;9:e113686.
43. Rossi A, Kontarakis Z, Gerri C, et al. Genetic compensation induced by deleterious mutations but not gene knockdowns. *Nature.* 2015;524:230.
44. Robu ME, Larson JD, Nasevicius A, et al. p53 Activation by knockdown technologies. *PLoS Genet.* 2007;3:e78.
45. Wride MA. Lens fibre cell differentiation and organelle loss: many paths lead to clarity. *Philos Trans R Soc Lond B Biol Sci.* 2011;366:1219-1233.
46. Qin Y, Zhao J, Min X, et al. MicroRNA-125b inhibits lens epithelial cell apoptosis by targeting p53 in age-related cataract. *Biochim Biophys Acta.* 2014;1842:2439-2447.
47. Grey AC, Li L, Jacobs MD, Schey KL, Donaldson PJ. Differentiation-dependent modification and subcellular distribution of aquaporin-0 suggests multiple functional roles in the rat lens. *Differentiation.* 2009;77:70-83.
48. Greiling TMS, Clark JI. The transparent lens and cornea in the mouse and zebra fish eye. *Semin Cell Dev Biol.* 2008;19:94-99.
49. Tittle RK, Sze R, Ng A, et al. Uhrf1 and Dnmt1 are required for development and maintenance of the zebrafish lens. *Dev Biol.* 2011;350:50-63.
50. Shand J, Døving KB, Collin SP. Optics of the developing fish eye: comparisons of Matthiessen's ratio and the focal length of the lens in the black bream *Acanthopagrus butcheri* (Sparidae, Teleostei). *Vision Res.* 1999;39:1071-1078.
51. Zwaan J, Williams RM. Cataracts and abnormal proliferation of the lens epithelium in mice carrying the CatFr gene. *Exp Eye Res.* 1969;8:161-162.
52. Shiels A, Mackey D, Bassnett S, Al-Ghoul K, Kuszak J. Disruption of lens fiber cell architecture in mice expressing a chimeric AQP0-LTR protein. *FASEB J.* 2000;14:2207-2212.
53. Sakuragawa M, Kuwabara T, Kinoshita JH, Fukui HN. Swelling of the lens fibers. *Exp Eye Res.* 1975;21:381-394.
54. Cheng C, Nowak RB, Fowler VM. The lens actin filament cytoskeleton: diverse structures for complex functions. *Exp Eye Res.* 2017;156:58-71.